J Physiol 591.23 (2013) pp 5923–5937

The Journal of Physiology

Development of heart failure is independent of K^+ channel-interacting protein 2 expression

Tobias Speerschneider, Søren Grubb, Artina Metoska, Søren-Peter Olesen, Kirstine Calloe and Morten B. Thomsen

Danish National Research Foundation Centre for Cardiac Arrhythmia, Department of Biomedical Sciences, Faculty of Health and Medical Sciences, University of Copenhagen, Copenhagen, Denmark

Key points

- Previous studies have suggested that the K^+ channel auxiliary subunit K^+ channel-interacting protein 2 (KChIP2) serves as a regulator of cardiac remodelling leading to heart failure and increased risk of arrhythmias.
- The results presented here show that the progression of cardiac remodelling and heart failure induced by transverse aortic constriction follows a similar time course in wild-type and KChIP2$^{-/-}$ mice.
- Protein expression analysis shows that ventricular KChIP2 is significantly downregulated in heart failure in wild-type mice.
- The electrophysiological analysis reveals enlarged J and T wave amplitudes and lower vulnerability to pacing-induced ventricular arrhythmias in KChIP2$^{-/-}$ control mice compared to wild-type control mice. Heart failure in wild-type and KChIP2$^{-/-}$ mice prompted comparable prolongation of QT intervals and ventricular effective refractory periods.
- Collectively, these results demonstrate that KChIP2 does not influence the structural and functional development of heart failure. Moreover, in contrast to previously reported data, downregulation of KChIP2 expression in heart failure may reduce the risk of cardiac arrhythmia.

Abstract Abnormal ventricular repolarization in ion channelopathies and heart disease is a major cause of ventricular arrhythmias and sudden cardiac death. K^+ channel-interacting protein 2 (KChIP2) expression is significantly reduced in human heart failure (HF), contributing to a loss of the transient outward K^+ current (I_{to}). We aim to investigate the possible significance of a changed KChIP2 expression on the development of HF and proarrhythmia. Transverse aortic constrictions (TAC) and sham operations were performed in wild-type (WT) and KChIP2$^{-/-}$ mice. Echocardiography was performed before and every 2 weeks after the operation. Ten weeks post-surgery, surface ECG was recorded and we paced the heart *in vivo* to induce arrhythmias. Afterwards, tissue from the left ventricle was used for immunoblotting. Time courses of HF development were comparable in TAC-operated WT and KChIP2$^{-/-}$ mice. Ventricular protein expression of KChIP2 was reduced by 70% after 10 weeks TAC in WT mice. The amplitudes of the J and T waves were enlarged in KChIP2$^{-/-}$ control mice. Ventricular effective refractory period, RR, QRS and QT intervals were longer in mice with HF compared to sham-operated mice of either genotype. Pacing-induced ventricular tachycardia (VT) was observed in 5/10 sham-operated WT mice compared with 2/10 HF WT mice with HF. Interestingly, and contrary to previously published data, sham-operated KChIP2$^{-/-}$ mice were resistant to pacing-induced VT resulting in only 1/10 inducible mice. KChIP2$^{-/-}$ with HF mice had similar low vulnerability to inducible VT (1/9). Our results suggest that although KChIP2 is downregulated in HF, it is not orchestrating the development of HF. Moreover, KChIP2 affects ventricular repolarization

DOI: 10.1113/jphysiol.2013.263483

and lowers arrhythmia susceptibility. Hence, downregulation of KChIP2 expression in HF may be antiarrhythmic in mice via reduction of the fast transient outward K^+ current.

(Received 9 August 2013; accepted after revision 4 October 2013; first published online 7 October 2013)
Corresponding author M. B. Thomsen: Danish National Research Foundation Centre for Cardiac Arrhythmia, Department of Biomedical Sciences, Faculty of Health and Medical Sciences, University of Copenhagen, 3b Blegdamsvej, building 12.5.36, Copenhagen N, Denmark. Email: mbthom@sund.ku.dk

Abbreviations ECG, electrocardiogram; HF, heart failure; $I_{Ca,L}$, L-type Ca^{2+} current; $I_{to,f}$, fast transient outward K^+ current; $I_{to,s}$, slow transient outward K^+ current; KChIP2, K^+ channel-interacting protein 2; LV, left ventricle; TAC, transverse aortic constriction; vERP, ventricular effective refractory period; VPC, ventricular premature complex; VT, ventricular tachycardia; WT, wild-type.

Introduction

Heart failure (HF) is one of the leading causes of morbidity and mortality with a prevalence of 1–2% in Western societies and progressively increasing incidence in patients over 50 years of age (Mosterd & Hoes, 2007). The condition is characterized by the impairment of the heart to adequately supply blood to meet the demand of the body. In the early stage of heart disease, a decrease in cardiac output is compensated by hypertrophy of the ventricle and high sympathetic drive; however, in the presence of a continued stressor these mechanisms may fail to maintain cardiac output, cardiac function deteriorates and HF develops. Treatment options for end-stage HF are mainly palliative or merely slowing the relentless progression of symptoms. It is estimated that death in approximately half of HF patients is sudden and due to ventricular tachyarrhythmias (Podrid *et al.* 1992). Dysregulation of cardiac ion-channel subunits leading to abnormal ventricular repolarization contributes to a high risk of arrhythmias and sudden cardiac death in hypertrophy and HF (Tomaselli & Zipes, 2004; Nerbonne & Kass, 2005).

Voltage-gated K^+ (Kv) channel-mediated currents are important determinants of ventricular repolarization (Nerbonne, 2000). Functional Kv channels are assembled by four α-subunits, and during the last decade an increasing number of interacting partners and auxiliary subunits have been identified, all influencing current density, kinetics or trafficking of the channel-forming α-subunits (An *et al.* 2000; Nerbonne *et al.* 2001; Deschenes *et al.* 2002; Lundby *et al.* 2010; David *et al.* 2013). Although the abnormal ventricular electrophysiological profile in HF arises from a composite dysregulation of several ion channels, altered ventricular repolarization has repeatedly been associated with reductions in the Kv4-mediated transient outward current (Kaab *et al.* 1998; Nass *et al.* 2008; Cordeiro *et al.* 2012; Suzuki *et al.* 2012). In humans, the native transient outward potassium current (I_{to}) is mediated by Kv4.3 channels modulated by the potassium channel-interacting protein 2 (KChIP2; An *et al.* 2000; Deschenes *et al.* 2002) and probably other subunits (Lundby *et al.* 2010). In mice, I_{to} can be divided into a fast and a slow current component: Kv4.2 channels give rise to the fast inactivating and fast recovering $I_{to,f}$, whereas the slow component ($I_{to,s}$) with slower inactivation and slower recovery from inactivation is presumably governed by Kv1.4 (Nerbonne, 2000).

Ventricular expression of KChIP2 mRNA and protein is downregulated in patients with HF potentially underlying the reported loss of I_{to} (Radicke *et al.* 2006; Soltysinska *et al.* 2009). In experimental models of hypertrophy, KChIP2 has been reported to be reduced (Zicha *et al.* 2004; Jia & Takimoto, 2006; Wang *et al.* 2007); however, this is not a consistent observation (Zicha *et al.* 2004; Marionneau *et al.* 2008; Jin *et al.* 2010). *In vivo* gene transfer of KChIP2 attenuated the development of left ventricular hypertrophy in rats, suggesting a regulatory role of KChIP2 in cardiac remodelling (Jin *et al.* 2010). Recently, Foeger *et al.* (2013) determined that KChIP2 is required for stabilization of Kv4.2 protein and for generation of $I_{to,f}$. Absence of KChIP2 has previously been associated with increased susceptibility to ventricular arrhythmias in mice despite unaltered QT intervals and refractory periods *in vivo* (Kuo *et al.* 2001), whereas other studies have demonstrated the opposite: reductions or total elimination of Kv4 and $I_{to,f}$ is antiarrhythmic (London *et al.* 2007).

Recently, it has become clear that some auxiliary subunits are not exclusively associated with one single pore-forming unit, but can be part of several different ion–channel complexes. In line with this, we have shown that KChIP2 not only augments Kv4 currents expressed in heterologous cells (Lundby *et al.* 2010) and in cardiomyocytes (Thomsen *et al.* 2009*b*), but also increases native L-type calcium current ($I_{Ca,L}$) via interaction with the cytosolic N-terminus of Cav1.2 (Thomsen *et al.* 2009*a*,*c*; Grubb *et al.* 2012). Cardiac $I_{Ca,L}$ has an essential role in excitation–contraction coupling and the contractile impairment seen in HF is in part secondary to altered cellular calcium handling, resulting in impaired and dyssynchronous calcium release from the sarcoplasmic reticulum (Pogwizd *et al.* 2001), whereas calcium entry via $I_{Ca,L}$ (Bers *et al.* 2006) or channel expression (Marionneau *et al.* 2008) are generally not altered.

In the present study, we examined the role of KChIP2 in the development of HF in mice, and tested the influence of KChIP2 on vulnerability to pacing-induced arrhythmias in mice with healthy and failing hearts.

Methods

Ethical approval and experimental animals

This investigation conforms to *Directive 2010/63/EU of the European Parliament* and was carried out under a licence from The Ministry of Food, Agriculture and Fisheries, Copenhagen, Denmark. All experiments were performed using male C57BL6 (WT) and KChIP2$^{-/-}$ mice (Thomsen *et al.* 2009*b*). The KChIP2$^{-/-}$ line was backcrossed to a C57BL6 background for six generations and genotyped using DNA isolated from tail samples. Mice were provided food and water *ad libitum* and housed in a room kept at 22°C with a 12 h light/dark schedule. A total of 31 WT and 27 KChIP2$^{-/-}$ mice were used for the data presented in this study. Surgical anaesthetised was ensured by frequent toe pinching. Body temperature was kept at 37 ± 0.5°C during all procedures. At the end of the procedures, the mice were euthanised by cervical dislocation.

Genotyping

Genotyping of mice was performed using tail tips from WT and KChIP2$^{-/-}$ mice and tissue PCR kit (Extract-N-Amp, Sigma-Aldrich, MO, USA) according to the manufacturer's protocol. PCR was used to amplify KChIP2 and neomycin control using previously published primer sequences (Thomsen *et al.* 2009*a*). The amplified DNA was separated on a 1% agarose gel and visualized with ethidium bromide.

Induction of heart failure

Transverse aortic constriction (TAC) was performed to induce a pressure overload on the left ventricle and trigger a remodelling process towards HF. Mice (6 weeks of age) were anaesthetized with 2% isoflurane and intubated with a 22G venous cannula. The animals were subsequently ventilated at rate of 180 breaths min^{-1} using a pressure-controlled rodent ventilator (MicroVent 1, Hallowell EMC, MA, USA). The hair on the chest was removed, a small incision in the cutaneous tissue was made, and the muscle layers surrounding the first and second uppermost rib on the left side of the chest were carefully spread apart under a dissecting microscope. After isolation of the transverse aorta, a blunt 27-gauge needle was placed parallel to the aortic arch and a silk ligature was tightened around the needle and the aorta between the brachiocephalic artery and left common carotid artery. The needle was immediately removed after tying the ligature. The thorax was subsequently closed with an absorbable ligature. Sham operations were performed in parallel, where the ligature was placed loosely around the aorta. Postoperative analgesia included 5 mg kg^{-1} carprofen and 0.05 mg kg^{-1} buprenorphine.

Immunoblotting

Immunoblotting was performed on protein extracts purified from the ventricles of sham- and TAC-operated animals. The intact, beating heart was quickly excised from the anaesthetized animal and rinsed in ice-cold saline. The ventricles were isolated by a horizontal incision at the level of the base of the heart and immediately frozen in liquid nitrogen and stored at −80°C until use. Tissues were homogenized in ice-cold TE buffer (20 mM Tris + 1 mM EDTA) containing a freshly made cocktail of protease inhibitors (1 mM 4-(2-aminoethyl)-benzenesulfonyl fluoride, 0.8 μM aprotinin, 20 μM leupeptin, 40 μM bestatin, 15 μM pepstatin A, 14 μM E-64, 200 μM phenylmethylsulfonyl fluoride) using a Precellys homogenizer. The homogenates were transferred to 1.5 ml tubes and Triton X-100 added to a final concentration of 1%. After 2 h incubation at 4°C the homogenates were centrifuged for 10 min at 15,000 *g*, 4°C and the pellet was discarded. The protein content of the supernatant was measured by the Lowry DC assay (Bio-Rad Laboratories Inc., CA, USA). For Western blot analysis, 100 μg of protein was separated on a SDS-PAGE gel (4–15% Tris HCl) and transferred to 0.45 μm nitrocellulose membranes (GE Healthcare, Life Sciences, Brondby, Denmark). Membranes were subsequently saturated with 2.5% non-fat milk and probed with primary antibodies against KChIP2 (3.5 μg ml^{-1}; NeuroMab, CA, USA) or glyceraldehyde 3-phosphate dehydrogenase (GAPDH; 0.2 μg ml^{-1}; Sigma-Aldrich, MO, USA) overnight at room temperature. The primary antibodies were detected by secondary horseradish peroxidase-conjugated donkey anti-mouse antibodies (Jackson Immunosearch Laboratories, UK) and visualized on hyperfilm (Amersham Biosciences) after enhanced chemiluminescence staining (Supersignal West Pico Chemiluminescent detection system, Thermo Scientific, IL, USA). Band density was quantified by ImageJ software (US National Institutes of Health, MD, USA).

Echocardiographic phenotyping

Transthoracic echocardiography of the heart was performed with a linear 30 MHz transducer according to the manufacturer's instructions (Vevo 770, VisualSonics, Canada). Each mouse was anaesthetised with 2% isoflurane whilst placed on a heating pad in a supine position. Temperature, heart rate and respiratory rate were closely monitored throughout the procedure. The chest hair was

removed and aquasonic gel (Mærsk-Andersen, Denmark) was applied to the thorax surface to optimize visibility of the cardiac chambers.

Diastolic and systolic left ventricle (LV) wall thicknesses (LVWT) and inner diameter (LVID) were measured in M-mode, using the maximal and minimal cross-sectional diameter in a heart cycle at the level of the papillary muscle, and averaged from parasternal long-axis and short-axis view (Fig. 1). Care was taken to ensure that measurements were performed in periods without respiratory movements. Left ventricular end-diastolic volume (LVEDV) and end-systolic volume (LVESV) were calculated as $LVID^3 \times [7/(2.4 + LVID)]$ in diastole and systole, respectively. Stroke volume (SV), ejection fraction (EF) and cardiac output (CO) were calculated subsequently: SV = LVEDV – LVESV; EF = SV/LVEDV, and CO = SV × heart rate. Echocardiography was performed prior to surgery and every 2 weeks after surgery. Animals that were not used for additional experiments were killed at the completion of echocardiography and wet weights of whole heart, lungs and liver were measured.

In vivo electrophysiological testing

Six-lead surface electrocardiogram (ECG) was recorded using subcutaneous needle electrodes in anaesthetized mice 10 weeks after TAC or sham operations. Signals were recorded at 4 kHz and filtered using a high-pass setting of 0.3 Hz and a low-pass setting of 1 kHz. After 5 min of baseline, β-adrenergic stimulation was achieved by injection of isoproterenol (isoprenaline; 2 μg (g body weight)$^{-1}$, I.P.). ECG traces were analysed offline before and 3 min after isoproterenol administration. Averaged signal ECGs were generated by aligning R waves of >100 complexes from lead II and analysed manually for RR, PR, QRS and QT duration using LabChart7 (ADInstruments). The start of the J wave was defined by the onset of the positive deflection immediately after the QRS complex to the point where the deflection crosses the isoelectric line and turns into the T wave (Boukens *et al.* 2013). The end of the T wave was defined as the moment where the negative deflection returned to the isoelectric line. The amplitudes of the J and T waves were measured at the peak of the deviation from the isoelectric line.

Intracardiac pacing of the LV was performed 1–3 days after β-adrenergic challenge. Under the influence of 2% isoflurane, a 1.1F pacing catheter (EPR-800, ADInstruments) was advanced through a small incision in the brachiocephalic artery into the LV. Cardiac pacing tested the left ventricular effective refractory period (vERP) and the susceptibility to arrhythmias. Specifically, vERP was determined by applying nine paced beats (9 × S1) at a cycle length of 100 ms followed by a single paced beat (S2) at a cycle length of 20 ms that was sequentially increased in 1 ms steps until stimuli resulted in ventricular depolarization. vERP was defined as the longest S1–S2 interval that did not result in ventricular capture. Inducibility of ventricular arrhythmias was evaluated by an S2 extra-stimulation technique: nine paced beats (9 × S1) at a cycle length of 100 ms followed by 2, 3, or 6 extra-stimulations (S2) at cycle lengths between 20 and 100 ms. Ventricular premature complexes (VPCs) were defined as 1–3 beats and ventricular tachycardia (VT) as ≥4 consecutive beats. If VT was induced, stimulation was repeated twice to determine reproducibility.

Statistical analysis

Data are expressed as mean ± SEM. Differences were evaluated statistically by Student's *t* test or ANOVA followed by Student–Newman–Keuls *post hoc* test, when appropriate. Kaplan–Meier survival curves and the Gehan–Breslow–Wilcoxon test were used to analyse survival proportions. Arrhythmia vulnerability was analysed by logistic regression analysis which considers overall arrhythmia inducibility and the number of extrastimuli required to induce ventricular tachyarrhythmia. $P < 0.05$ was considered statistically significant.

Results

Comparable development of heart failure in WT and KChIP2$^{-/-}$ mice

To determine the role of KChIP2 in the disease progress towards HF, LV pressure overload was applied in WT and KChIP2$^{-/-}$ mice. Transthoracic echocardiography of the heart was performed prior to surgery and every 2 weeks after surgery (Fig. 1*A*). Transverse aortic constriction in WT mice caused a gradual decrease in left ventricular ejection fraction over 10 weeks when compared with sham-operated controls (from 64 ± 1 to 30 ± 3%, $P < 0.05$; Fig. 1*B*). Left ventricular wall thickness was increased 2 weeks after TAC operation and remained stable thereafter (Fig. 1*C*), whereas left ventricular volume showed progressive dilatation (Fig. 1*D*). This cardiac dilatation and reduction in function demonstrated the presence of HF in mice 10 weeks after TAC. Surprisingly, development of HF in KChIP2$^{-/-}$ mice followed a similar time course to that of WT mice (Fig. 1). Moreover, mortality was increased by TAC but the Kaplan–Meier survival analysis revealed no significant impact on survival in the absence of KChIP2 (Fig. 1*E*).

In WT and KChIP2$^{-/-}$ mice with HF, heart rates were increased by 19% and 17%, respectively, yet cardiac outputs were reduced in both groups secondary to a decline in stroke volume (Table 1). Heart weights and lung weights were increased in WT and KChIP2$^{-/-}$ mice with HF relative to controls, whereas body weights were

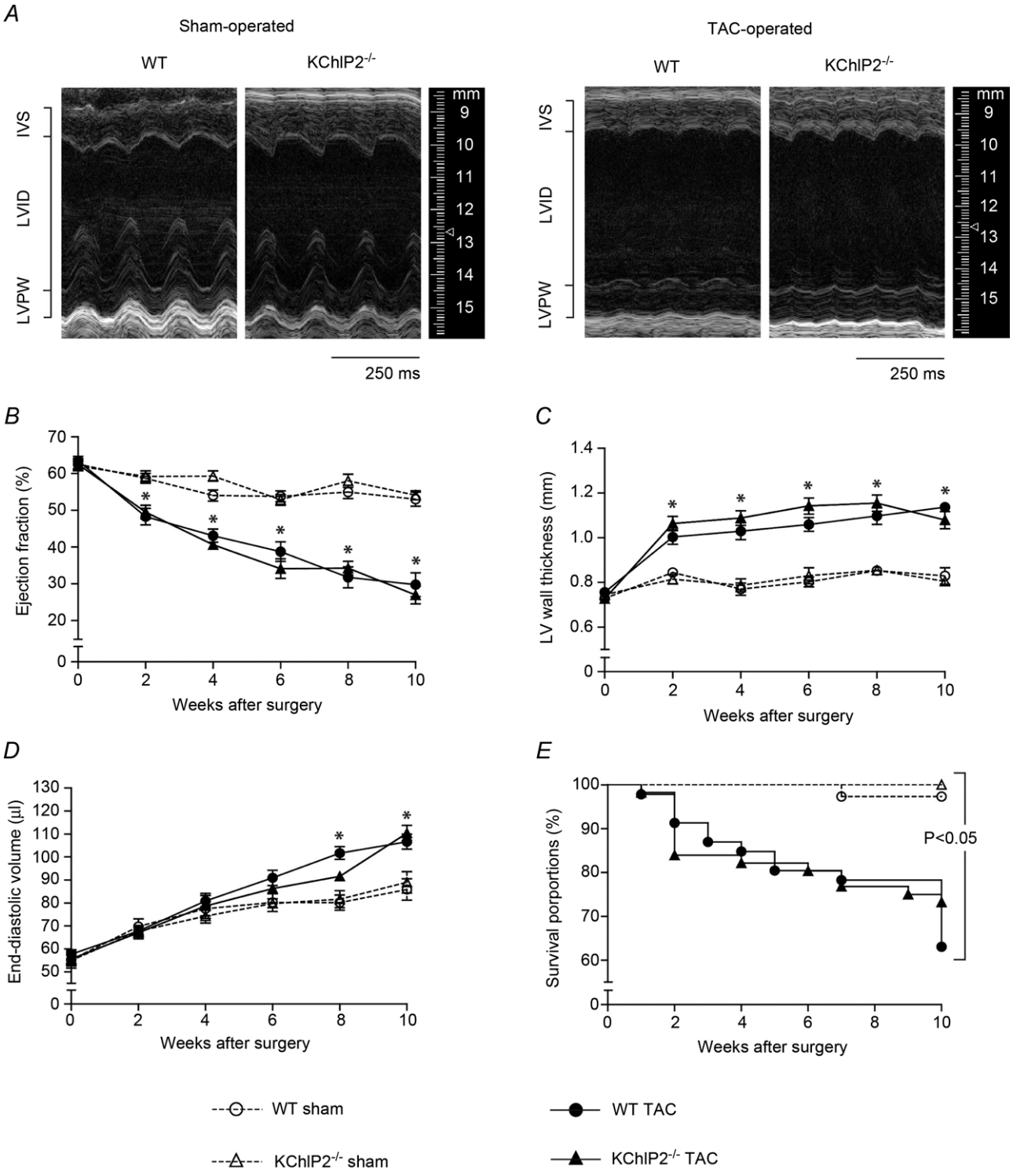

Figure 1. Development of HF is comparable in WT and KChIP2$^{-/-}$ mice after TAC
A, representative M-mode images of the LV short-axis view from anaesthetized WT and KChIP2$^{-/-}$ mice with and without HF. LV inner diameter (LVID) and thickness of the LV posterior wall (LVPW) and interventricular septum (IVS) are measured in short- and long-axis view in systole and diastole to determine mean wall thickness and to estimate LV volumes. *B*, LV ejection fraction was determined as stroke volume relative to end-diastolic volume. Prior to surgery, there were no differences in ejection fraction, and sham operations in WT ($n = 9$) and KChIP2$^{-/-}$ ($n = 10$) mice caused no significant change in ejection fraction during the 10 week follow-up. In contrast, TAC in WT ($n = 10$) and KChIP2$^{-/-}$ ($n = 8$) mice induced a marked reduction in cardiac function already at 2 weeks and

Table 1. Echocardiographic and postmortem examination of WT and KChIP2$^{-/-}$ mice with and without HF

	WT sham	KChIP2$^{-/-}$ sham	WT HF	KChIP2$^{-/-}$ HF
n	9	10	10	8
Heart rate (beats min^{-1})	435 ± 12	439 ± 13	519 ± 11*	512 ± 9*
Stroke volume (μl)	45 ± 2	48 ± 3	30 ± 2*	29 ± 2*
Cardiac output (ml min^{-1})	20 ± 1	21 ± 2	16 ± 1*	15 ± 1*
Body weight (g)	32 ± 1	33 ± 1	29 ± 1*	30 ± 1*
Heart weight (mg)	235 ± 21	243 ± 19	408 ± 30*	363 ± 28*
Lung weight (mg)	187 ± 13	177 ± 14	419 ± 51*	423 ± 67*

All values are means ± SEM; *n*, number of mice; *$P < 0.05$ *versus* sham.

lower in HF mice irrespective of genotype (Table 1). Liver-to-body-weight ratio was comparable among all mice indicating a preserved right ventricular function (data not shown). Ventricular KChIP2 protein levels were reduced by ∼70% in WT mice with HF relative to controls, while the protein was not detectable in KChIP2$^{-/-}$ mice (Fig. 2).

Altered repolarization in KChIP2$^{-/-}$ mice

Next, we evaluated the *in vivo* electrophysiological and proarrhythmic consequences of KChIP2 deletion in mice with healthy and failing hearts. Murine ventricular depolarization and repolarization displayed a temporal overlap producing a conjoined QRS complex and J wave on the ECG (Fig. 3*A* and *B*). The duration of the QRS complex and QT interval were similar in the sham-operated WT and KChIP2$^{-/-}$ mice (Fig. 3*C*). The JT segment was biphasic with an immediate, positive J wave and a prolonged negative T wave (Fig. 3*B*). As shown previously (Kuo *et al.* 2001; Thomsen *et al.* 2009*c*), the positive J wave had a significantly larger amplitude in KChIP2$^{-/-}$ mice compared to WT mice (0.20 ± 0.02 mV *versus* 0.13 ± 0.02 mV, $P < 0.05$; Fig. 3*B*). In addition, we found that the amplitude of the negative T wave was larger in the KChIP2$^{-/-}$ mice compared to the WT mice (−53 ± 3 μV *versus* −25 ± 9 μV, $P < 0.05$). In HF, QRS and QT intervals were prolonged (Fig. 3*C*), as expected, and the JT segment was entirely negative (Fig. 3*B*). The electrocardiographic analysis did not reveal any differences between WT and KChIP2$^{-/-}$ mice with HF.

Since stimulation of β-adrenergic receptors may unmask potential arrhythmia vulnerability, we injected a high dose of isoproterenol into anaesthetized mice (Shusterman *et al.* 2010). In sham-operated mice, β-adrenergic stimulation increased the heart rate by ∼50%; however, this response was significantly blunted in HF irrespective of genotype (Fig. 4*A*). No VPC or VT was observed in any mice following β-adrenergic stimulation. The JT segment became entirely positive in all mice under the influence of isoproterenol (Fig. 4*B*), and due to frequently inseparable J and T waves, and P waves superimposing final ventricular repolarization in mice with HF, we chose to measure the amplitude of the JT segment 30 ms after the peak of the R wave, rather than the duration of the waveforms. The amplitude of the JT segment measured here was significantly smaller in β-adrenergically stimulated sham-operated KChIP2$^{-/-}$ mice compared to the sham-operated WT mice (4 ± 13 μV *versus* 52 ± 13 μV, $P < 0.05$). In contrast, β-adrenergic stimulation in the mice with HF did not reveal different amplitudes of the JT segment in the WT and KChIP2$^{-/-}$ (115 ± 16 μV *versus* 94 ± 35 μV, $P > 0.05$).

Presence of KChIP2 confers vulnerability to pacing-induced arrhythmias

To further explore the potential proarrhythmic consequences of altered electrophysiology and HF, we measured ventricular effective refractory period (vERP) and tested arrhythmia susceptibility *in situ*

culminated in HF with an ejection fraction below 30% at the 10 week time point in WT and KChIP2$^{-/-}$ mice. The time courses of development of HF in WT and KChIP2$^{-/-}$ mice are practically superimposable. *C*, LV wall thickness, determined by 4 independent measurements in each mouse at each time point, is illustrated for the 4 groups of mice. As is evident, the LV wall thickness is increased in TAC-operated WT and KChIP2$^{-/-}$ mice from 2 to 10 weeks, whereas no temporal changes in wall thickness are identified in sham-operated WT and KChIP2$^{-/-}$ mice. *D*, mean LV end-diastolic volume was estimated from a single measurement of LV inner diameter in short- and long-axis views and was increased after 8 and 10 weeks after TAC in WT and KChIP2$^{-/-}$ mice. *$P < 0.05$ for both WT and KChIP2$^{-/-}$ *versus* the respective sham group. *E*, Kaplan–Meier survival curve illustrating overall survival based on surgery and genotype. As shown, the Kaplan–Meier curves begin to diverge at 2 weeks and continue to diverge for the remainder of the study; however, the curves for TAC-operated WT and KChIP2$^{-/-}$ mice are comparable.

(Fig. 5*A*). Ventricular ERP and the occurrence of pacing-induced ventricular premature complexes (VPCs) were comparable in WT and KChIP2$^{-/-}$ controls (Fig. 5*B*). In mice with HF, vERP was significantly prolonged and pacing-induced VPCs were more frequent, irrespective of genotype (Fig. 5*B*). Interestingly, the KChIP2$^{-/-}$ control mice were less vulnerable to pacing-induced VT compared to WT control mice (Fig. 5*A*). Overall, pacing-induced VT was present in 5/10 sham WT control mice compared to only 1/10 VT in KChIP2$^{-/-}$ control mice (Fig. 5*C*; $P < 0.05$). The mean VT duration was 448 ± 43 ms in WT control mice with a mean cycle length of 61 ± 5 ms ($n = 5$). The presence of HF in the WT mice reduced the arrhythmia vulnerability, but HF in the KChIP2$^{-/-}$ mice did not change the low VT inducibility. The low numbers of VT in the latter groups preclude a meaningful characterization of the arrhythmias in these mice. No spontaneous episodes of arrhythmias were observed in any mice.

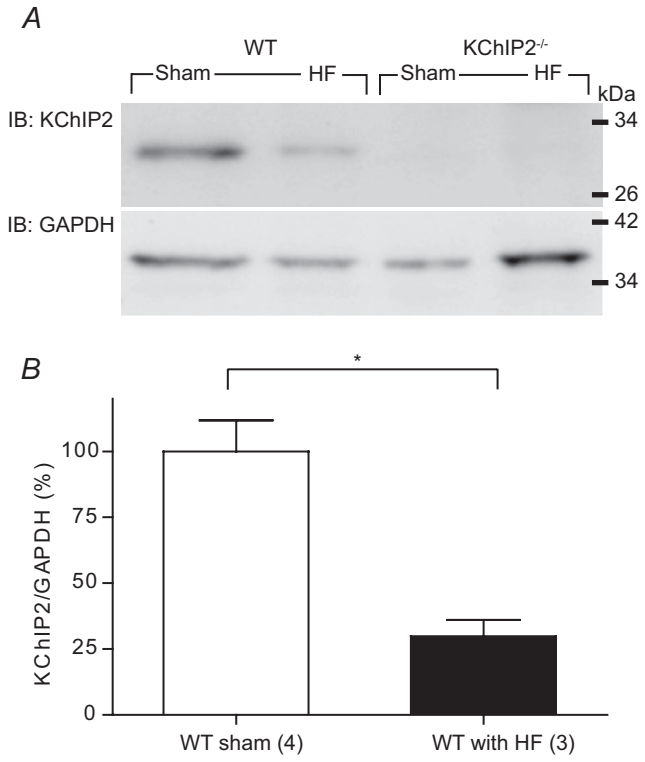

Figure 2. Ventricular KChIP2 expression is down-regulated in HF
Ten weeks after surgery, KChIP2 protein levels from isolated ventricles were measured by immunoblotting (IB). GAPDH expression levels were measured simultaneously and used to control equal loading. *A*, representative immunoblot showing clear expression of ventricular KChIP2 in WT sham-operated mice and reduced expression in WT mice with HF. KChIP2 expression was absent in the KChIP2$^{-/-}$ mice. *B*, densitometric quantification of immunoblot bands shows reduced KChIP2 expression by 70 ± 6% in WT mice with heart failure. Number of hearts indicated in brackets. *$P < 0.05$.

Discussion

Role of KChIP2 and I_{to} expression in development of HF

Similar to previous studies on haemodynamic remodelling in mice after TAC (Boulaksil *et al.* 2010; Shi *et al.* 2013), the results of the experiments reported here demonstrate that left ventricular function is depressed after several weeks of pressure overload. Interestingly, we find that cardiac remodelling and deterioration of pump function follow similar time courses in WT and KChIP2$^{-/-}$ mice, thus indicating that the progression of HF is independent of KChIP2. Virally mediated overexpression of KChIP2 in rats subjected to aortic banding for 8 days augments Kv4.2 and Kv4.3 expression, increases total I_{to} and prevents hypertrophy by increasing the expression of the Na^+–Ca^{2+} exchanger and reducing calcineurin activation (Jin *et al.* 2010). Endogenous KChIP2 levels in control hypertrophic rats were not decreased, corroborating our results that KChIP2 reduction is not an initiating event in cardiac remodelling in rodents. In combination, these studies suggest that KChIP2 downregulation is a marker for the transition from compensated hypertrophy to deteriorating HF.

The reports on the haemodynamic consequences of eliminating or reducing the $I_{to,f}$ current in mice seem conflicting. Cardiac-specific expression of a dominant-negative pore-mutant of Kv4.2 (Kv4.2W362F) in C57CBA mice leads to total elimination of I_{to}, but does not alter heart-to-body weight ratios or produce any histological dissimilarities (Barry *et al.* 1998). In another approach to target I_{to}, cardiac-specific expression of a dominant-negative N-terminal fragment of Kv.4.2 in B6XCBAF2 mice also leads to removal of I_{to}, but only in a subset of cardiomyocytes from young animals (Wickenden *et al.* 1999). Moreover, cardiac hyper-contractility, increased blood pressure, and an augmented $I_{Ca,L}$ caused larger cytosolic calcium transients and activation of calcineurin (Sah *et al.* 2002). Adult mice expressing the protein fragment spontaneously developed HF and loss of I_{to} in all myocytes (Wickenden *et al.* 1999). It is speculated that cellular toxicity induced by overexpression of the protein fragment, impact of background strain and/or calcineurin activation may underlie the discrepancy between the phenotypic characteristics in the two mouse strains (Folco *et al.* 1997; Wickenden *et al.* 1999; Nerbonne *et al.* 2001). In a third study, Kv4.2$^{-/-}$ in FVB mice results in elimination of $I_{to,f}$ and compensatory upregulation of $I_{to,s}$ without evidence of ventricular hypertrophy or myocardial dysfunction (Guo *et al.* 2005). Taken together with the present study showing normal haemodynamic function and no signs of structural remodelling in sham-operated KChIP2$^{-/-}$ mice, these results suggest that loss of $I_{to,f}$ is not a triggering event initiating a continuing decline of the pumping activity of

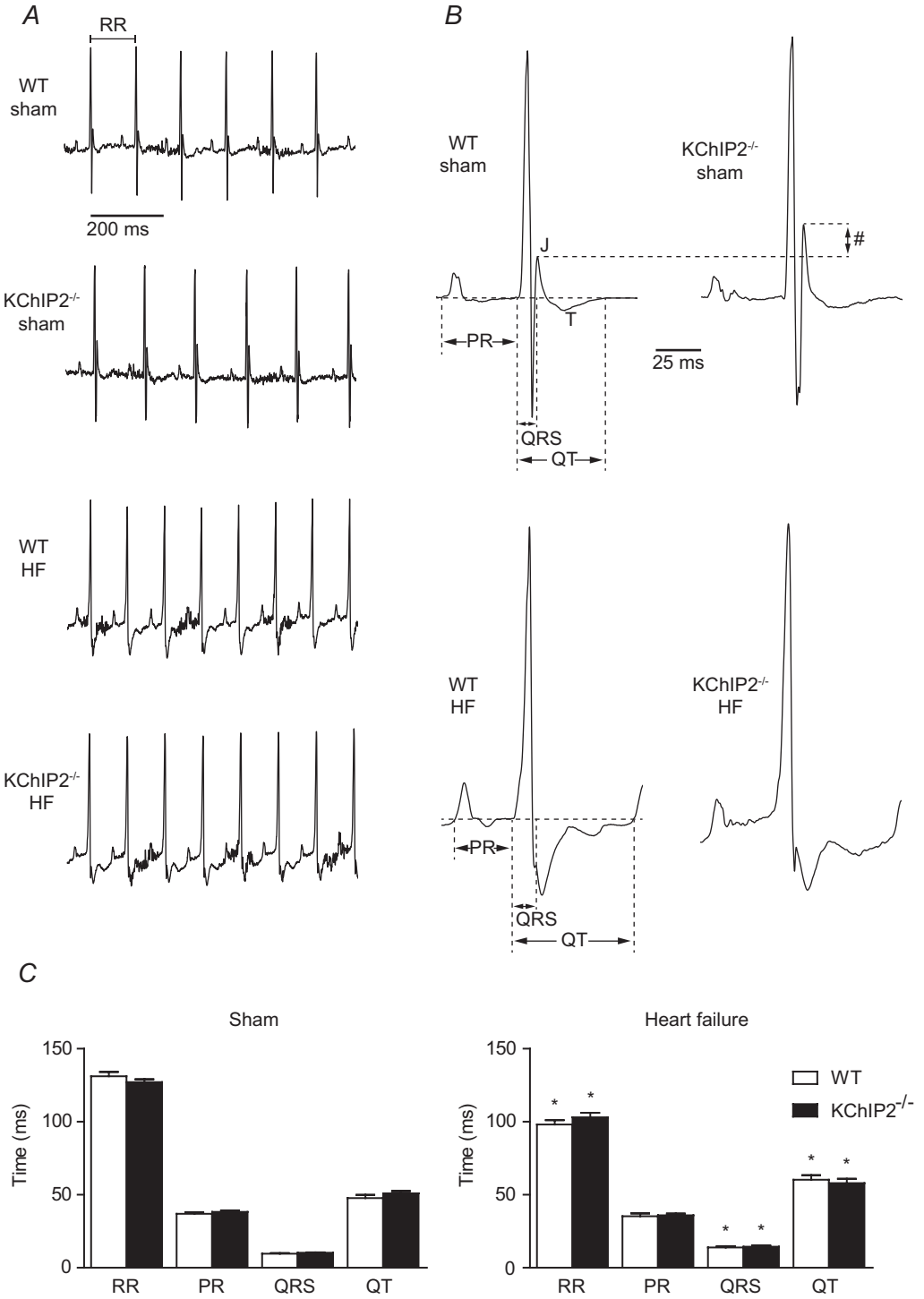

Figure 3. Electrocardiographic phenotyping reveals increased J wave and T wave amplitudes in KChIP2$^{-/-}$ mice without HF

A, unprocessed, representative surface ECG traces (lead II) obtained from sham-operated WT and KChIP2$^{-/-}$ mice with and without HF. *B*, averaged ECG traces were generated by aligning ECG complexes after the R wave and averaging the signal. This analysis revealed increased J wave (#) and T wave amplitudes in sham-operated KChIP2$^{-/-}$ mice compared to WT mice. WT and KChIP2$^{-/-}$ mice with HF presented entirely negative JT segments. *C*, sham-operated WT ($n = 10$) and KChIP2$^{-/-}$ mice ($n = 10$) showed similar RR, PR, QRS and QT intervals. When HF was induced, WT ($n = 9$) and KChIP2$^{-/-}$ mice ($n = 8$) presented a significantly shorter RR interval and prolongation of the QRS and QT intervals compared to sham-operated mice (*$P < 0.05$). However, no difference was observed in the measured ECG parameters of WT and KChIP2$^{-/-}$ mice with HF.

the heart, as seen in HF. Rather, loss of I_{to} and down-regulation of KChIP2 is a consequence of HF.

Altered electrophysiological parameters after loss of KChIP2

We have previously shown that KChIP2 augments $I_{Ca,L}$ density by interacting with the N-terminal inhibitory segment of the pore-forming α_{1C} subunit (Thomsen *et al.* 2009*c*). Recently, we and others have confirmed these findings (Grubb *et al.* 2012; Foeger *et al.* 2013). In the present study, we find that baseline ventricular contractility is not changed in KChIP2$^{-/-}$ mice suggesting the presence of a contractile adaptation to reduced $I_{Ca,L}$ in these mice. KChIP2$^{-/-}$ leads to complete loss of Kv4.2 protein despite maintained

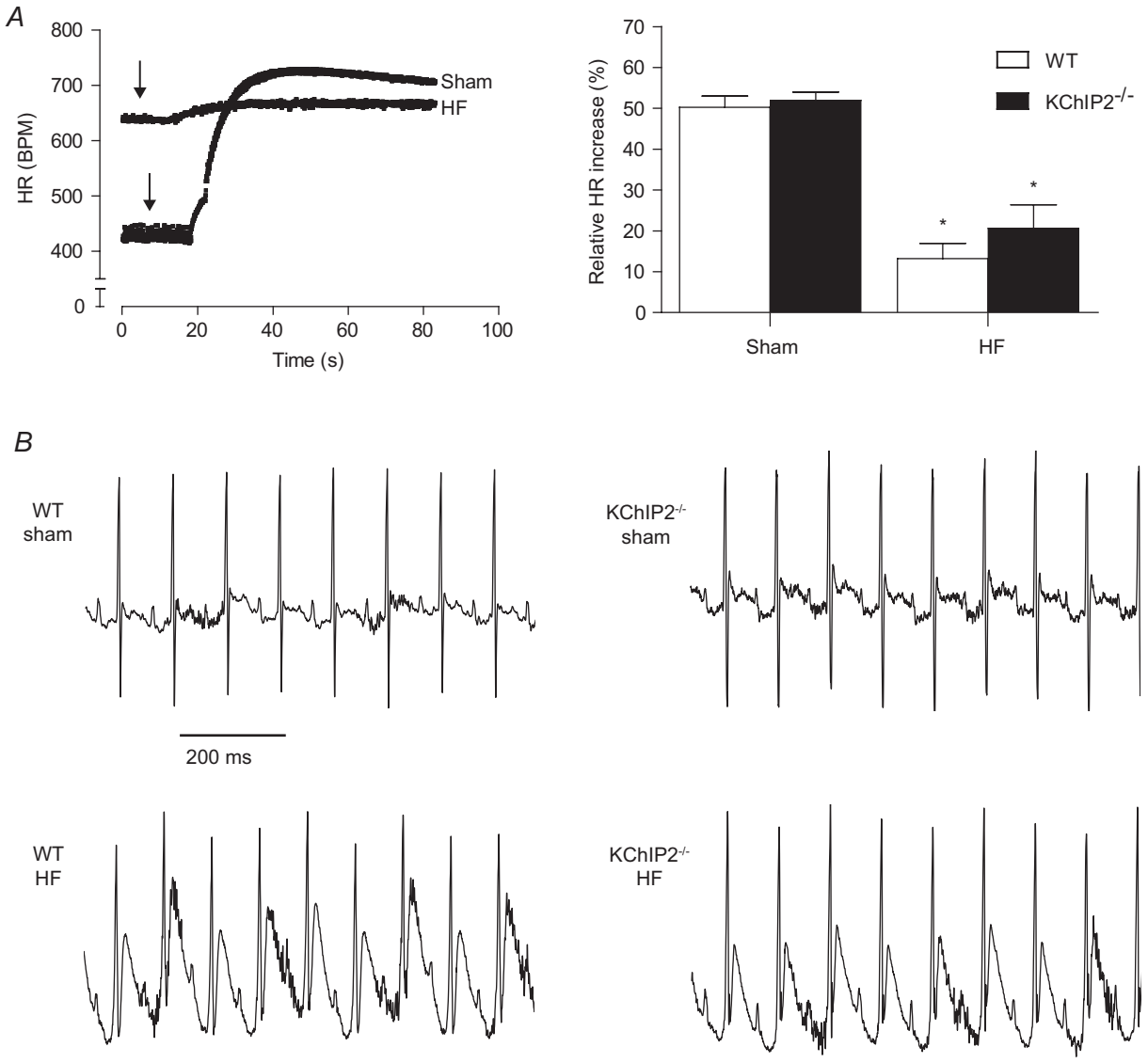

Figure 4. β-Adrenergic stimulation produces a blunted increase in heart rate in WT and KChIP2$^{-/-}$ mice with HF; however, no arrhythmias are observed
A, left, representative examples of the development of heart rate (HR) after injection of 2 μg g^{-1} isoproterenol I.P. (arrows) in a sham-operated WT mouse and a WT mouse with HF. BPM, beats per minute. All mice in HF had elevated resting heart rates. Right, cumulative data showing that WT ($n = 9$) and KChIP2$^{-/-}$ mice ($n = 8$) in HF exhibited a blunted response to β-adrenergic stimulation compared to sham-operated WT ($n = 10$) and KChIP2$^{-/-}$ ($n = 10$) controls. The chronotropic response to isoproterenol was not affected by the presence of KChIP2 in sham or HF. *B*, unprocessed representative surface ECG traces (lead II) obtained from sham-operated WT and KChIP2$^{-/-}$ mice with and without HF 3 min after isoproterenol injection. β-Adrenergic stimulation produced positive JT segments in all mice. All mice with HF showed larger, positive JT segment amplitudes upon β-adrenergic stimulation than sham-operated mice. There was no difference, however, between the genotypes. *$P < 0.05$ *versus* sham.

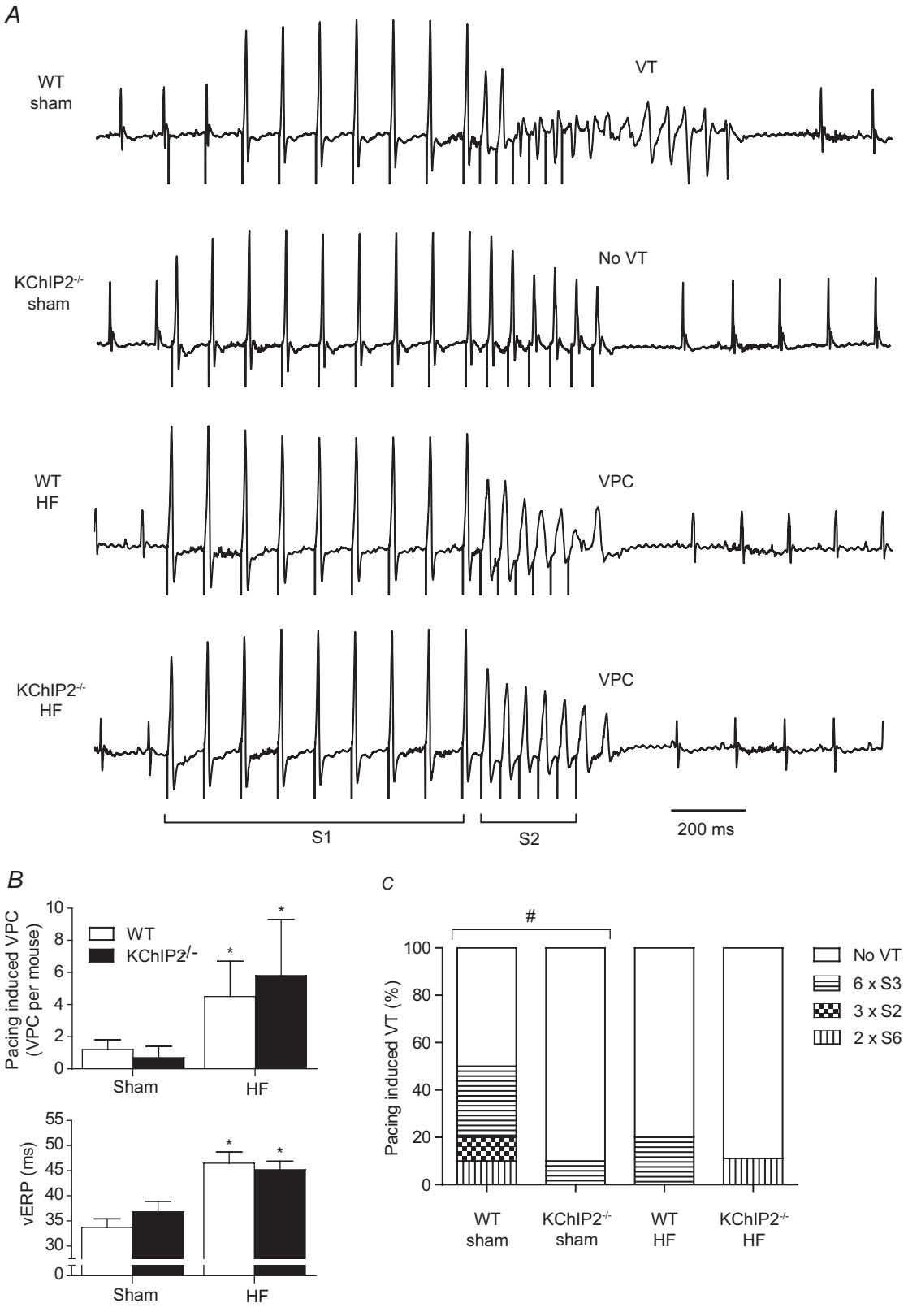

Figure 5. KChIP2$^{-/-}$ mice without HF show a lower vulnerability to pacing-induced arrhythmias
A, we inserted a 1.1F pacing catheter in the left ventricle of all mice to perform an *in vivo* electrophysiological test of arrhythmia vulnerability. Unprocessed representative surface ECG traces (lead II) during programmed electrical stimulation of the LV from sham-operated WT mice and KChIP2$^{-/-}$ mice, and WT and KChIP2$^{-/-}$ with HF. The

(Foeger *et al.* 2013) or even increased (Thomsen *et al.* 2009*b*) mRNA levels for the protein, demonstrating that KChIP2 is pivotal in the stabilization of the endogenous $I_{to,f}$ channel protein complex in ventricular cardiomyocytes.

The electrocardiographic analysis of the present study revealed larger amplitudes of positive J waves and negative T waves in KChIP2$^{-/-}$ mice, but unaltered QT intervals. Previously, Kuo *et al*. (2001) also reported normal QT intervals and *prolonged duration of elevated ST segment* in conscious KChIP2$^{-/-}$ mice. The elevated ST segment is equivalent to the augmented J wave of the present study. These two findings are in apparent conflict with the report by Foeger *et al*. (2013) that ECG waveforms are unaffected by loss of KChIP2; however, the findings could reflect differences in the choice of anaesthetic approach (Huneke *et al.* 2004). Foeger *et al.* (2013) used the injectable anaesthetic tribromoethanol for their *in vivo* electrophysiological studies, whereas we used isoflurane inhalation anaesthesia. Isoflurane anaesthesia induces modest prolongation of the RR interval in WT mice, which is not seen with tribromoethanol (Petric *et al.* 2012). Murine QT intervals are shortened to comparable levels by the two anaesthetics. It is possible that small differences in RR intervals or direct effects of tribromoethanol or isoflurane on J and T wave amplitudes account for the differences between the present study and that of Foeger and colleagues (2013).

ECG waveforms in HF animals were significantly different compared to sham-operated controls. A well-known compensatory physiological reflex to reduced stroke volume is an increased heart rate, which is also observed in the present study by a dramatic reduction in RR intervals. The JT segment was entirely negative and QT intervals were prolonged, corroborating earlier studies by Shi *et al.* (2013) on TAC-operated WT mice. As expected, we observed no differences in ECG waveforms in the presence of HF between WT and KChIP2$^{-/-}$ animals, where KChIP2 is significantly reduced and eliminated, respectively.

KChIP2$^{-/-}$ mice without HF are protected from pacing-induced ventricular arrhythmia

Stimulation of the β_1-adrenergic receptors leads to elevated levels of cAMP, activation of several kinases, predominantly protein kinase A, and the phosphorylation of target proteins. Phosphorylation of the $I_{Ca,L}$ macromolecular complex increases current amplitude and contributes to increased contractility in the fight-or-flight response (Lundby *et al.* 2013). I_{to} is reduced in the presence of α-adrenergic agonists (Homma *et al.* 2000); however, based on the absence of reports it seems probable that I_{to} is not modulated by β_1-adrenergic stimulation. In the present study, β_1-adrenergic stimulation was used to generate a potentially proarrhythmic condition, by increasing the depolarizing $I_{Ca,L}$ in the setting of a reduced repolarization reserve (Roden, 1998; Thomsen *et al.* 2004) in the KChIP2$^{-/-}$ mice. Heart rate was increased and T waves were enlarged in all four groups of mice, but no arrhythmias were observed, suggesting that repolarization reserve is sufficiently strong in these mice to prevent the triggering of proarrhythmic events under the present circumstances.

In order to further test arrhythmia vulnerability, we delivered triggering stimuli by intracardiac electrical pacing to determine if the electrophysiological substrate was present. We observed that WT mice without HF are more vulnerable to pacing-induced VT compared to KChIP2$^{-/-}$ mice, which appears to be in conflict with the findings reported by Kuo *et al*. (2001) that KChIP2$^{-/-}$ mice are highly susceptible to arrhythmias, despite unaltered vERP. It is presently unclear what underlies the difference in arrhythmia outcome; however, we speculate that differences in background strain, sex, age or anaesthesia may contribute to the conflicting arrhythmia outcome. In the present study, we used a pure C57BL6 background strain of male mice at 16 weeks of age under isoflurane anaesthesia, whereas Kuo *et al*. (2001) used a mixed 129SV and Black Swiss background, pentobarbital anaesthesia and did not report sex or age. The influence of background strain on cardiac function and

protocol used consisted of a pacing train of 9 stimuli (S1) with 100 ms cycle length, followed by 1–6 short-coupled extra stimuli (S2) of incremental interpulse interval. *B*, the numbers of ventricular premature complexes (VPC) per mouse observed after any pacing protocol were similar in sham-operated WT ($n = 10$) and KChIP2$^{-/-}$ mice ($n = 10$). The presence of HF increased the number of VPCs per mouse (*$P < 0.05$ *versus* sham); however, there were no differences between the WT ($n = 10$) and KChIP2$^{-/-}$ ($n = 9$) mice. Ventricular ERP in WT and KChIP2$^{-/-}$ mice were comparable in control and equally prolonged at HF (#$P < 0.05$ *versus* sham). *C*, interestingly, sham-operated KChIP2$^{-/-}$ mice showed a lower vulnerability to pacing-induced ventricular tachycardia (VT) compared to WT sham-operated mice (#$P < 0.05$). Vulnerability to VT was low in HF. Arrhythmia vulnerability is indicated as the percentage of mice in the group susceptible to VT by 2, 3 or 6 S2 extra stimuli. Arrhythmia vulnerability was statistically compared by logistic regression analysis which considers overall arrhythmia inducibility and the number of extra stimuli required to induce ventricular tachycardia.

electrophysiology has been investigated previously by Shah *et al.* (2010). In their study, they demonstrate that 129SV cardiomyocytes are smaller and have a lower t-tubular density compared to C57BL6 cardiomyocytes. Moreover, sarcoplasmic reticulum calcium load is larger in SV129 cardiomyocytes. It is presently unclear whether these differences are sufficient to explain the marked differences in proarrhythmia between the two studies. Not only were 8 of 12 KChIP2$^{-/-}$ mice susceptible to pacing-induced ventricular arrhythmia in the study by Kuo *et al.* (2001), the WT mice were completely protected from arrhythmia (0 of 10 mice). This is in sharp contrast to the present findings; however, we do not consider our data surprising: based on previous work in mice with genetic ablation of $I_{to,f}$ (Brunner *et al.* 2001; London *et al.* 2007), we expected that deletion of KChIP2 and the resulting loss of $I_{to,f}$ would be antiarrhythmic, not proarrhythmic, in mice. Kuo *et al.* (2001) suggested that elimination of the transmural gradient of $I_{to,f}$ by KChIP2$^{-/-}$ would potentially increase ventricular heterogeneity of repolarization in the mouse and that this would confer the susceptibility to VT. However, Kv4.2DN mice have highly homogeneous repolarization times throughout the ventricle, with virtually no apex–base gradient of repolarization (London *et al.* 2007). $I_{to,f}$ is heterogeneously expressed in the mammalian heart: it is significantly higher in the right ventricle compared to the left ventricle, and within the left ventricle, $I_{to,f}$ is higher in the apex than at the base of the ventricle. In addition, $I_{to,f}$ is lower in the endocardial wall than at the epicardial surface of the ventricle (Brunet *et al.* 2004; Patel & Campbell, 2005). These gradients are consistent with mRNA levels for both Kv4.2 and KChIP2 (Teutsch *et al.* 2007). In addition to the marked reduction in dispersion of repolarization in the Kv4.2DN mouse, VT was not readily inducible by electrical stimulation in these animals (Brunner *et al.* 2001). Thus, loss of $I_{to,f}$, whether mediated by elimination of Kv4.2 or KChIP2, leads to a homogeneous repolarization time throughout the heart which reduces arrhythmia vulnerability in mice. It is outside the scope of the present study to determine the underlying culprit for the observed arrhythmia susceptibility in the report by Kuo *et al.* (2001).

Auxiliary protein subunits modulate Kv4.2 to generate $I_{to,f}$

Kv4.2 associates with KChIP2 and potentially a number of additional auxiliary proteins to generate native $I_{to,f}$. Simultaneous expression of Kv4, dipeptidylpeptidase 6 and KChIP2 mimics I_{to} from the heart (Radicke *et al.* 2005); however, members of the KCNE family may also modulate the current (Lundby *et al.* 2010). Neuronal calcium sensor protein 1 regulates Kv4 current, especially in the immature heart (Nakamura *et al.* 2001,2003). Finally, Kvβ, traditionally thought to associate with Kv1 channels, or Navβ, the accessory subunit from the cardiac sodium channel, modulate Kv4-mediated current in heterologous expression systems (Deschenes & Tomaselli, 2002), yet the relative physiological importance of these protein interactions remains to be determined. The elegant studies by Foeger and colleagues demonstrate a reciprocal stabilization of Kv4 and KChIP2 proteins, and shows that in the absence of KChIP2, $I_{to,f}$ is eliminated (Foeger *et al.* 2010, 2013). Hence, potential compensatory remodelling of these other subunits would affect currents other than $I_{to,f}$ in KChIP2$^{-/-}$ mice. An in-depth analysis of the influence of these additional auxiliary subunits in mice with HF is yet to be determined.

Limitations

Approximately 25% of TAC-operated mice died during the 10 weeks of development of HF (Fig. 1*D*). We have no data determining whether these deaths occurred as a consequence of ventricular pump failure or arrhythmia, and whether ventricular pacing in these mice would have resulted in VT. A high susceptibility to arrhythmia in the failing heart is primarily associated with the early stages of HF, rather than late stages (Lane *et al.* 2005). It is possible that intracardiac pacing to induce arrhythmias would have been more successful if performed earlier than at end-stage HF at 10 weeks.

Caution should be taken when translating these findings into clinical use due to the marked difference in ionic currents underlying ventricular depolarization and repolarization in man and mouse. The murine ventricular action potential is relatively short compared to the human, where I_{to} constitutes the notch between the spike and the dome in the action potential (Calloe *et al.* 2011).

Conclusions

Although KChIP2 downregulation is a molecular hallmark in HF, this study indicates that KChIP2 does not affect the structural and functional development of the disease. Nevertheless, the absence of KChIP2 affects cardiac repolarization by increasing J and T wave amplitudes on the ECG and lowering arrhythmia vulnerability. Hence, downregulation of KChIP2 expression in HF may have an antiarrhythmic effect in mice by reducing $I_{to,f}$.

References

An WF, Bowlby MR, Betty M, Cao J, Ling HP, Mendoza G, Hinson JW, Mattsson KI, Strassle BW, Trimmer JS & Rhodes KJ (2000). Modulation of A-type potassium channels by a family of calcium sensors. *Nature* **403**, 553–556.

Barry DM, Xu H, Schuessler RB & Nerbonne JM (1998). Functional knockout of the transient outward current, long-QT syndrome, and cardiac remodeling in mice expressing a dominant-negative Kv4 α subunit. *Circ Res* **83**, 560–567.

Bers DM, Despa S & Bossuyt J (2006). Regulation of Ca^{2+} and Na^{+} in normal and failing cardiac myocytes. *Ann N Y Acad Sci* **1080**, 165–177.

Boukens BJ, Hoogendijk MG, Verkerk AO, Linnenbank A, van Dam P, Remme CA, Fiolet JW, Opthof T, Christoffels VM & Coronel R (2013). Early repolarization in mice causes overestimation of ventricular activation time by the QRS duration. *Cardiovasc Res* **97**, 182–191.

Boulaksil M, Noorman M, Engelen MA, van Veen TA, Vos MA, de Bakker JM & van Rijen HV (2010). Longitudinal arrhythmogenic remodelling in a mouse model of longstanding pressure overload. *Neth Heart J* **18**, 509–515.

Brunet S, Aimond F, Li H, Guo W, Eldstrom J, Fedida D, Yamada KA & Nerbonne JM (2004). Heterogeneous expression of repolarizing, voltage-gated K^{+} currents in adult mouse ventricles. *J Physiol* **559**, 103–120.

Brunner M, Guo W, Mitchell GF, Buckett PD, Nerbonne JM & Koren G (2001). Characterization of mice with a combined suppression of I_{to} and $I_{K,slow}$. *Am J Physiol Heart Circ Physiol* **281**, H1201–H1209.

Calloe K, Nof E, Jespersen T, Di Diego JM, Chlus N, Olesen SP, Antzelevitch C & Cordeiro JM (2011). Comparison of the effects of a transient outward potassium channel activator on currents recorded from atrial and ventricular cardiomyocytes. *J Cardiovasc Electrophysiol* **22**, 1057–1066.

Cordeiro JM, Calloe K, Moise NS, Kornreich B, Giannandrea D, Di Diego JM, Olesen SP & Antzelevitch C (2012). Physiological consequences of transient outward K^{+} current activation during heart failure in the canine left ventricle. *J Mol Cell Cardiol* **52**, 1291–1298.

David JP, Andersen MN, Olesen SP, Rasmussen HB & Schmitt N (2013). Trafficking of the I_{Ks}-complex in MDCK cells: site of subunit assembly and determinants of polarized localization. *Traffic* **14**, 399–411.

Deschenes I, DiSilvestre D, Juang GJ, Wu RC, An WF & Tomaselli GF (2002). Regulation of Kv4.3 current by KChIP2 splice variants: a component of native cardiac I_{to}? *Circulation* **106**, 423–429.

Deschenes I & Tomaselli GF (2002). Modulation of Kv4.3 current by accessory subunits. *FEBS Lett* **528**, 183–188.

Foeger NC, Marionneau C & Nerbonne JM (2010). Co-assembly of Kv4 α subunits with K^{+} channel-interacting protein 2 stabilizes protein expression and promotes surface retention of channel complexes. *J Biol Chem* **285**, 33413–33422.

Foeger NC, Wang W, Mellor RL & Nerbonne JM (2013). Stabilization of Kv4 protein by the accessory K^{+} channel interacting protein 2 (KChIP2) subunit is required for the generation of native myocardial fast transient outward K^{+} currents. *J Physiol* **591**, 4149–4166.

Folco E, Mathur R, Mori Y, Buckett P & Koren G (1997). A cellular model for long QT syndrome. Trapping of heteromultimeric complexes consisting of truncated Kv1.1 potassium channel polypeptides and native Kv1.4 and Kv1.5 channels in the endoplasmic reticulum. *J Biol Chem* **272**, 26505–26510.

Grubb S, Calloe K & Thomsen MB (2012). Impact of KChIP2 on cardiac electrophysiology and the progression of heart failure. *Front Physiol* **3**, 118.

Guo W, Jung WE, Marionneau C, Aimond F, Xu H, Yamada KA, Schwarz TL, Demolombe S & Nerbonne JM (2005). Targeted deletion of Kv4.2 eliminates $I_{to,f}$ and results in electrical and molecular remodeling, with no evidence of ventricular hypertrophy or myocardial dysfunction. *Circ Res* **97**, 1342–1350.

Homma N, Hirasawa A, Shibata K, Hashimito K & Tsujimoto G (2000). Both α_{1A}- and α_{1B}-adrenergic receptor subtypes couple to the transient outward current (I_{To}) in rat ventricular myocytes. *Br J Pharmacol* **129**, 1113–1120.

Huneke R, Fassl J, Rossaint R & Luckhoff A (2004). Effects of volatile anesthetics on cardiac ion channels. *Acta Anaesthesiol Scand* **48**, 547–561.

Jia Y & Takimoto K (2006). Mitogen-activated protein kinases control cardiac KChIP2 gene expression. *Circ Res* **98**, 386–393.

Jin H, Hadri L, Palomeque J, Morel C, Karakikes I, Kaprielian R, Hajjar R & Lebeche D (2010). KChIP2 attenuates cardiac hypertrophy through regulation of I_{to} and intracellular calcium signaling. *J Mol Cell Cardiol* **48**, 1169–1179.

Kaab S, Dixon J, Duc J, Ashen D, Nabauer M, Beuckelmann DJ, Steinbeck G, McKinnon D & Tomaselli GF (1998). Molecular basis of transient outward potassium current downregulation in human heart failure: a decrease in Kv4.3 mRNA correlates with a reduction in current density. *Circulation* **98**, 1383–1393.

Kuo HC, Cheng CF, Clark RB, Lin JJ, Lin JL, Hoshijima M, Nguyen-Tran VT, Gu Y, Ikeda Y, Chu PH, Ross J, Giles WR & Chien KR (2001). A defect in the Kv channel-interacting protein 2 (KChIP2) gene leads to a complete loss of I_{to} and confers susceptibility to ventricular tachycardia. *Cell* **107**, 801–813.

Lane RE, Cowie MR & Chow AW (2005). Prediction and prevention of sudden cardiac death in heart failure. *Heart* **91**, 674–680.

London B, Baker LC, Petkova-Kirova P, Nerbonne JM, Choi BR & Salama G (2007). Dispersion of repolarization and refractoriness are determinants of arrhythmia phenotype in transgenic mice with long QT. *J Physiol* **578**, 115–129.

Lundby A, Andersen MN, Steffensen AB, Horn H, Kelstrup CD, Francavilla C, Jensen LJ, Schmitt N, Thomsen MB & Olsen JV (2013). In vivo phosphoproteomics analysis reveals the cardiac targets of β-adrenergic receptor signaling. *Sci Signal* **6**, rs11.

Lundby A, Jespersen T, Schmitt N, Grunnet M, Olesen SP, Cordeiro JM & Calloe K (2010). Effect of the I_{to} activator NS5806 on cloned K_v4 channels depends on the accessory protein KChIP2. *Br J Pharmacol* **160**, 2028–2044.

Marionneau C, Brunet S, Flagg TP, Pilgram TK, Demolombe S & Nerbonne JM (2008). Distinct cellular and molecular mechanisms underlie functional remodeling of repolarizing K^+ currents with left ventricular hypertrophy. *Circ Res* **102**, 1406–1415.

Mosterd A & Hoes AW (2007). Clinical epidemiology of heart failure. *Heart* **93**, 1137–1146.

Nakamura TY, Pountney DJ, Ozaita A, Nandi S, Ueda S, Rudy B & Coetzee WA (2001). A role for frequenin, a Ca^{2+}-binding protein, as a regulator of Kv4 K^+-currents. *Proc Natl Acad Sci U S A* **98**, 12808–12813.

Nakamura TY, Sturm E, Pountney DJ, Orenzoff B, Artman M & Coetzee WA (2003). Developmental expression of NCS-1 (frequenin), a regulator of Kv4 K^+ channels, in mouse heart. *Pediatr Res* **53**, 554–557.

Nass RD, Aiba T, Tomaselli GF & Akar FG (2008). Mechanisms of disease: ion channel remodeling in the failing ventricle. *Nat Clin Pract Cardiovasc Med* **5**, 196–207.

Nerbonne JM (2000). Molecular basis of functional voltage-gated K^+ channel diversity in the mammalian myocardium. *J Physiol* **525**, 285–298.

Nerbonne JM & Kass RS (2005). Molecular physiology of cardiac repolarization. *Physiol Rev* **85**, 1205–1253.

Nerbonne JM, Nichols CG, Schwarz TL & Escande D (2001). Genetic manipulation of cardiac K^+ channel function in mice: what have we learned, and where do we go from here? *Circ Res* **89**, 944–956.

Patel SP & Campbell DL (2005). Transient outward potassium current, 'I_{to}', phenotypes in the mammalian left ventricle: underlying molecular, cellular and biophysical mechanisms. *J Physiol* **569**, 7–39.

Petric S, Clasen L, van Wessel C, Geduldig N, Ding Z, Schullenberg M, Mersmann J, Zacharowski K, Aller MI, Schmidt KG & Donner BC (2012). *In vivo* electrophysiological characterization of TASK-1 deficient mice. *Cell Physiol Biochem* **30**, 523–537.

Podrid PJ, Fogel RI & Fuchs TT (1992). Ventricular arrhythmia in congestive heart failure. *Am J Cardiol* **69**, 82G–95G; discussion 95G–96G.

Pogwizd SM, Schlotthauer K, Li L, Yuan W & Bers DM (2001). Arrhythmogenesis and contractile dysfunction in heart failure: Roles of sodium-calcium exchange, inward rectifier potassium current, and residual β-adrenergic responsiveness. *Circ Res* **88**, 1159–1167.

Radicke S, Cotella D, Graf EM, Banse U, Jost N, Varro A, Tseng GN, Ravens U & Wettwer E (2006). Functional modulation of the transient outward current I_{to} by KCNE β-subunits and regional distribution in human non-failing and failing hearts. *Cardiovasc Res* **71**, 695–703.

Radicke S, Cotella D, Graf EM, Ravens U & Wettwer E (2005). Expression and function of dipeptidyl-aminopeptidase-like protein 6 as a putative β-subunit of human cardiac transient outward current encoded by Kv4.3. *J Physiol* **565**, 751–756.

Roden DM (1998). Taking the "idio" out of "idiosyncratic": predicting torsades de pointes. *Pacing Clin Electrophysiol* **21**, 1029–1034.

Sah R, Oudit GY, Nguyen TT, Lim HW, Wickenden AD, Wilson GJ, Molkentin JD & Backx PH (2002). Inhibition of calcineurin and sarcolemmal Ca^{2+} influx protects cardiac morphology and ventricular function in K_v4.2N transgenic mice. *Circulation* **105**, 1850–1856.

Shah AP, Siedlecka U, Gandhi A, Navaratnarajah M, Al-Saud SA, Yacoub MH & Terracciano CM (2010). Genetic background affects function and intracellular calcium regulation of mouse hearts. *Cardiovasc Res* **87**, 683–693.

Shi C, Wang X, Dong F, Wang Y, Hui J, Lin Z, Yang J & Xu Y (2013). Temporal alterations and cellular mechanisms of transmural repolarization during progression of mouse cardiac hypertrophy and failure. *Acta Physiol (Oxf)* **208**, 95–110.

Shusterman V, McTiernan CF, Goldberg A, Saba S, Salama G & London B (2010). Adrenergic stimulation promotes T-wave alternans and arrhythmia inducibility in a TNF-α genetic mouse model of congestive heart failure. *Am J Physiol Heart Circ Physiol* **298**, H440–H450.

Soltysinska E, Olesen SP, Christ T, Wettwer E, Varro A, Grunnet M & Jespersen T (2009). Transmural expression of ion channels and transporters in human nondiseased and end-stage failing hearts. *Pflugers Arch* **459**, 11–23.

Suzuki T, Shioya T, Murayama T, Sugihara M, Odagiri F, Nakazato Y, Nishizawa H, Chugun A, Sakurai T, Daida H, Morimoto S & Kurebayashi N (2012). Multistep ion channel remodeling and lethal arrhythmia precede heart failure in a mouse model of inherited dilated cardiomyopathy. *PLoS One* **7**, e35353.

Teutsch C, Kondo RP, Dederko DA, Chrast J, Chien KR & Giles WR (2007). Spatial distributions of Kv4 channels and KChip2 isoforms in the murine heart based on laser capture microdissection. *Cardiovasc Res* **73**, 739–749.

Thomsen MB, Foster E, Nguyen KH & Sosunov EA (2009*a*). Transcriptional and electrophysiological consequences of KChIP2-mediated regulation of Ca_V1.2. *Channels (Austin)* **3**, 308–310.

Thomsen MB, Sosunov EA, Anyukhovsky EP, Özgen N, Boyden PA & Rosen MR (2009*b*). Deleting the accessory subunit KChIP2 results in loss of $I_{to,f}$ and increased $I_{K,slow}$ that maintains normal action potential configuration. *Heart Rhythm* **6**, 370–377.

Thomsen MB, Verduyn SC, Stengl M, Beekman JDM, de Pater G, van Opstal J, Volders PGA & Vos MA (2004). Increased short-term variability of repolarization predicts *d*-sotalol-induced torsades de pointes in dogs. *Circulation* **110**, 2453–2459.

Thomsen MB, Wang C, Ozgen N, Wang HG, Rosen MR & Pitt GS (2009*c*). Accessory subunit KChIP2 modulates the cardiac L-type calcium current. *Circ Res* **104**, 1382–1389.

Tomaselli GF & Zipes DP (2004). What causes sudden death in heart failure? *Circ Res* **95**, 754–763.

Wang Y, Cheng J, Chen G, Rob F, Naseem RH, Nguyen L, Johnstone JL & Hill JA (2007). Remodeling of outward K+ currents in pressure-overload heart failure. *J Cardiovasc Electrophysiol* **18**, 869–875.

Wickenden AD, Lee P, Sah R, Huang Q, Fishman GI & Backx PH (1999). Targeted expression of a dominant-negative K_v4.2 K^+ channel subunit in the mouse heart. *Circ Res* **85**, 1067–1076.

Zicha S, Xiao L, Stafford S, Cha TJ, Han W, Varro A & Nattel S (2004). Transmural expression of transient outward potassium current subunits in normal and failing canine and human hearts. *J Physiol* **561**, 735–748.

Additional information

Competing interests

None declared.

Author contributions

All experiments were performed at the University of Copenhagen. T.S. contributed to the conception and design of the experiments, the collection, analysis and interpretation of data, and to writing the manuscript. S.G. and A.M. contributed to the collection, analysis and interpretation of data. S.-P.O. and K.C. contributed to the conception and design of the experiments and interpretation of data. M.B.T. contributed to the conception and design of the experiments, the collection, analysis and interpretation of data, and to writing the manuscript. All authors have contributed through critical review of the intellectual content of the manuscript and all have approved the submitted version.

Funding

This work was supported by The Danish Heart Foundation (grant numbers: 11-04-R84-A3357-22639 to T.S. and 12-04-R90-A4017-22721 to S.G.); The Danish Agency for Science, Technology and Innovation, Medical Research Council (grant number 10-084244 to M.B.T.) and the Danish National Research Foundation Centre for Cardiac Arrhythmia.

Acknowledgements

The technical support of Amer Mujezinovic is greatly appreciated.

Author's present address

K. Calloe: Department of Veterinary Clinical and Animal Science, Faculty of Health and Medical Sciences, University of Copenhagen, Copenhagen, Denmark.